Chapter 3

Molecular Modeling

3.1. Introduction

In this study pharmacophore models will be created to screen a virtual library of FDA approved drugs for compounds that may inhibit MAO-A and MAO-B. The virtual library of approved drugs will be obtained from the DrugBank and the screening of this library will be carried out with the molecular modeling software, Discovery Studio 3.1. The steps that will be followed may be summarized as follows:

- Using X-ray crystal structures of MAO-A and MAO-B with ligands co-crystallized in their respective active sites, structure-based pharmacophore models will be generated.
- The interactions of the co-crystallized ligands with MAO-A and MAO-B will be analyzed to gain insight into interactions that are important for inhibitor binding.
- The abilities of the models to distinguish between known MAO-A and MAO-B inhibitors and compounds known not to bind to these enzymes will be determined using a test set of known inhibitors and compounds known not to bind to the MAOs.
- Different conformations of the drugs within the virtual library of FDA approved drugs will be generated.
- The conformers will be mapped to the pharmacophore models and the hits identified.
- Selected hits will be docked into the active sites of MAO-A and MAO-B to gain insight into their binding modes.
- Selected hits will be evaluated *in vitro* as inhibitors of MAO-A and MAO-B.

3.2. Experimental methods

3.2.1. Construction and screening of the pharmacophore models

As mentioned in the previous chapter, structure-based pharmacophore generation is dependent on the availability of the target protein structures. In this study three structure-based pharmacophore models were constructed using the following structures:

- the X-ray crystal structure of human MAO-A with harmine co-crystallized in the active site (PDB code: 2Z5X).
- the X-ray crystal structure of human MAO-B with safinamide co-crystallized in the active site (PDB code: 2V5Z).

The following steps were followed:

(a) Protein Preparation

- The crystallographic structures of the MAOs (as given above), were retrieved from the Brookhaven Protein Data Bank (www.rcsb.org/pdb).
- The correctness of the valences of the FAD cofactors (oxidized state) and cocrystallized ligands were verified and the protein models were automatically typed with the Momany and Rone CHARMm forcefield
- With the tools provided in Discovery Studio, the pH was set to 7.4 and hydrogen atoms were added to the FAD co-factor and the co-crystallized ligands.
- The pKa values and protonation states of the ionizable amino acids were calculated and hydrogen atoms were added at pH 7.4 to the protein models.
- A fixed atom constraint was applied to the backbone of the enzymes and the models were energy minimized using the Smart Minimizer algorithm with the maximum steps set to 50 000. For this procedure the implicit generalized Born solvation model with molecular volume was used.

(b) Pharmacophore construction

- All crystal waters were deleted from the protein models, except those which undergo hydrogen bonding with the co-crystallized ligands, and the binding sites of the MAOs were defined, based on the location of the ligands.
- To determine important interactions between the co-crystallized ligands and amino acid residues and water molecules, an interaction map between the ligands and amino acid residues was calculated.
- Based on the interaction analysis, pharmacophore features were added to the model. The acceptor, donor and hydrophobic features were clustered in turn. Location constraints were added to the features.
- A shape constraint was added to the co-crystallized ligand.

(c) Pharmacophore validation and library screening

- After the Pharmacophore models had been constructed, test sets were constructed. The test sets consisted of ligands which do not inhibit the MAOs and ligands which do have MAO-A and MAO-B inhibition activity. Conformations of the test sets were generated (250 of each ligand) by using the BEST conformation method.
- The generated conformations were then queried by the pharmacophore models to determine which conformations fit the features best.

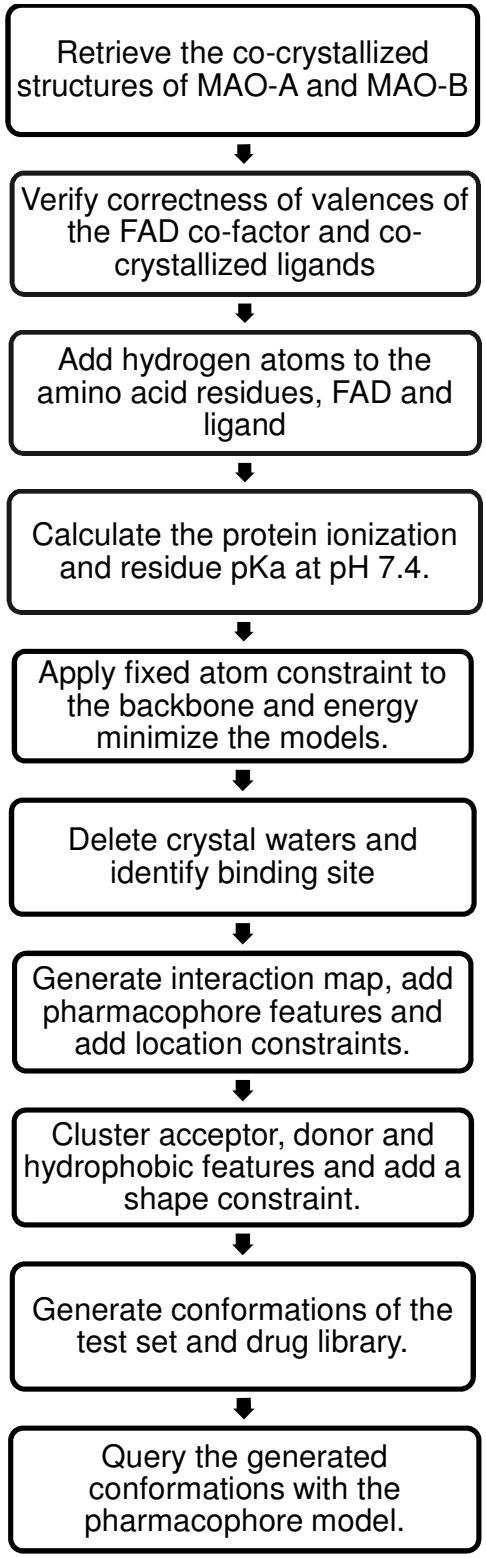

Figure 3.1. Workflow for the construction of a structure-based pharmacophore model and screening of a virtual library.

3.2.2. Molecular docking

- The molecular docking was carried out with Discovery studio 3.1. The crystallographic structure of MAO-A and MAO-B were retrieved from the Brookhaven Protein Data Bank. The following structures were used for these studies:
    - MAO-A co-crystallized with harmine (pdb file 2Z5X)
    - MAO-B co-crystallized with safinamide (pdb file 2V5Z)

(a) Protein Preparation

- The protonation states of the ionizable amino acid residues were calculated at pH 7.4 and hydrogen atoms were added to the receptor model.
- The valence of the FAD co-factor (oxidized state) and co-crystallized ligands were corrected and hydrogen atoms were added according to the appropriate protonation states at pH 7.4. The structures were typed automatically with the Momany and Rone CHARMm forcefield.
- A fixed atom constraint was applied to the backbone of the enzymes and the models were energy minimized using the Smart Minimizer algorithm with the maximum steps set to 50 000. For this procedure the implicit generalized Born solvation model with molecular volume was used.
- The X-ray crystallographic structures of MAO-B, show that three active site water molecules are conserved. Thus for both MAO-A and MAO-B, the crystal water molecules were removed with the exception of these three active site waters. The crystal waters, which occupy the analogous positions in the MAO-A active site compared to those cited above for MAO-B, were retained.

(b) Docking

- The co-crystallized ligands and the backbone constraints were subsequently removed from the models and the binding sites were identified by a floodfilling algorithm.
- Structures of the ligands to be docked were constructed within Discovery studio, and their hydrogen atoms were added according to the appropriate protonation states at pH 7.4. The geometries of the ligands were briefly optimized in Discovery studio using a fast Dreiding-like forcefield (1000 interactions) and the atom potential types and partial charges were assigned with the Momany and Rone CHARMm forcefield.
- Docking of the ligands was carried out with CDOCKER algorithm with the generation of 10 random ligand conformations and a heating target temperature of 700 K in full potential mode.
- The docking solutions were refined using the Smart Minimizer algorithm. Ten possible binding solutions were computed for each docked ligand and the best-ranked binding conformation of each ligand was determined according to the DockScore values.

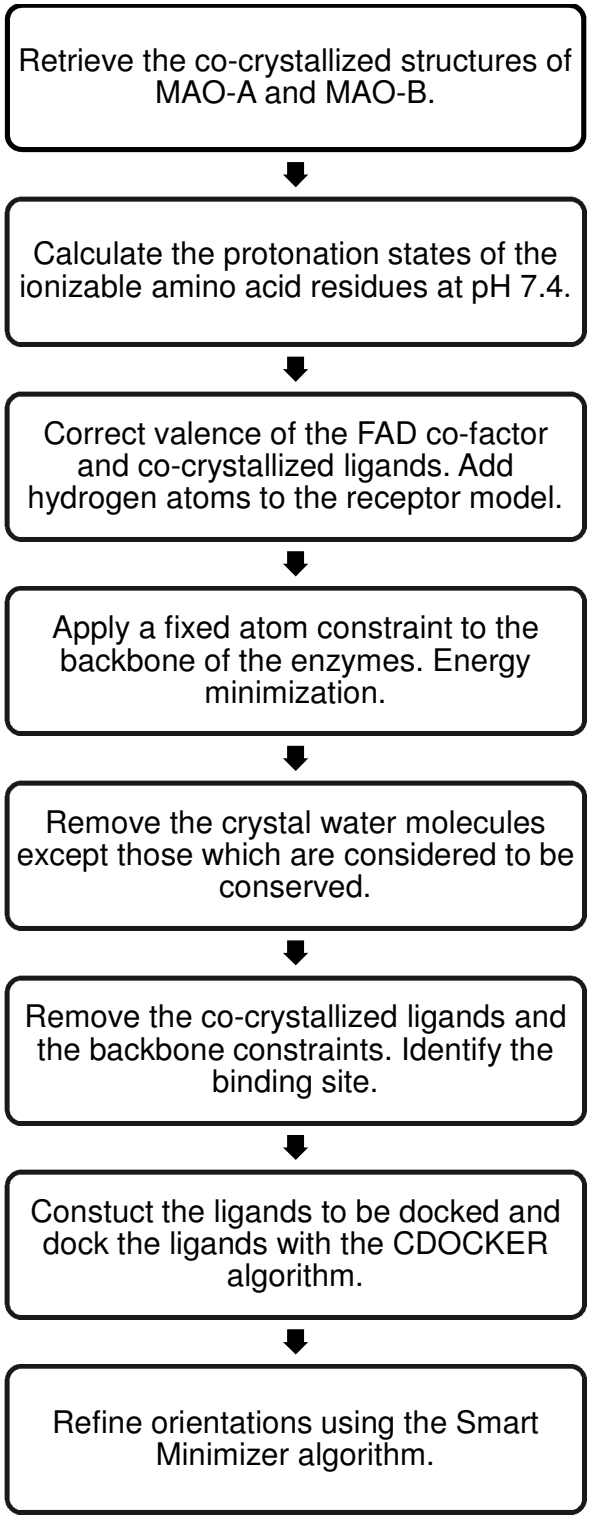

Figure 3.2. Workflow for docking ligands into the active sites of the MAOs.

3.3. Results

3.3.1. Structure-based pharmacophore of MAO-A

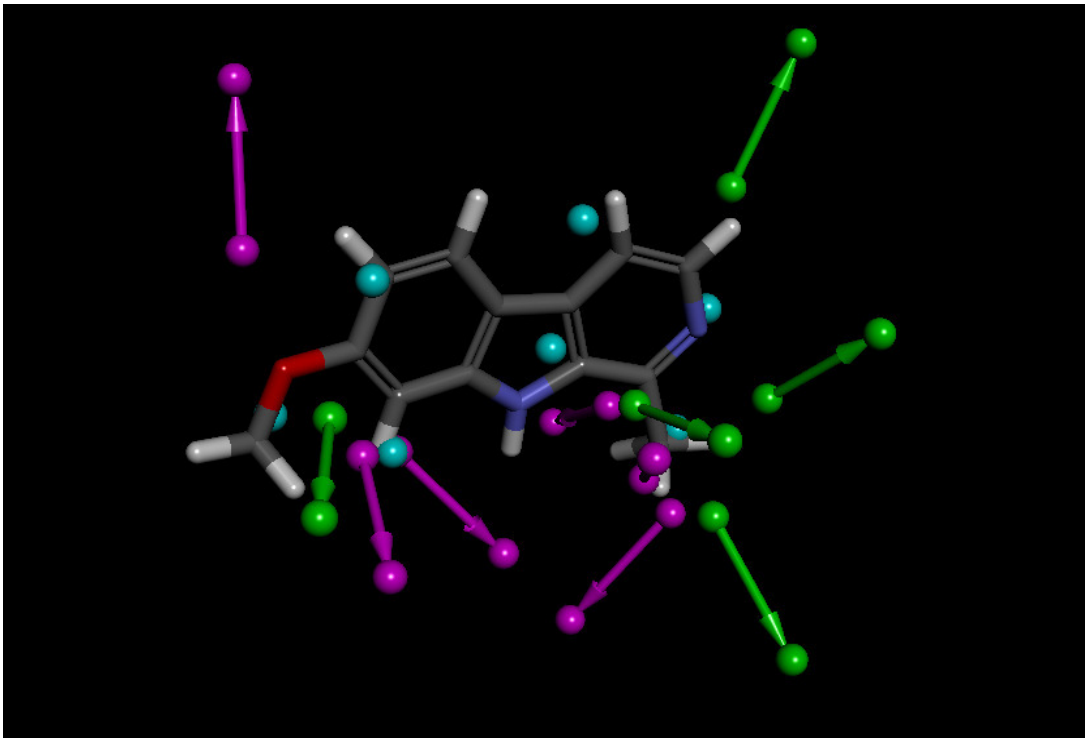

Figure 3.3. Graphical representation of the pharmacophore model derived from the structure of harmine using the *structure-based* approach. This model may be used to screen a virtual library for structures that bind to MAO-A. The green arrows represent hydrogen bond acceptor features, the purple arrows represent hydrogen bond donor features and the cyan spheres represent hydrophobic features.

For the construction of this pharmacophore model (Fig. 3.3), the X-ray crystal structure of human MAO-A with harmine co-crystallized in the active site was used (PDB code: 2Z5X). All calculations were carried out with Discovery Studio 3.1. The software firstly calculated the interactions between harmine and the amino acid residues and water molecules of the active site. The software also determines additional interactions which may exist between a ligand and the MAO-A active site. Based on these possible interactions pharmacophore features are placed in the active site. These features are hydrogen bond acceptor features, hydrogen bond donor features and hydrophobic

features. The user then clusters the features into groups. With this step a group of features that represents the same interactions are combined into a single feature. Location constraints are subsequently added to each feature. These are spheres which are placed around the features (at center) and define the ideal location for the ligand atom(s). The sphere represents the tolerance of the allowable deviation of the ligand atom(s) from the ideal position. In the last step, a shape feature is placed around harmine (Fig. 3.4). When searching a virtual database for ligands that may map to the pharmacophore model, the algorithm attempts to fill up the shape, not just have the structure fit inside it. Since harmine is a relatively large inhibitor and fills the MAO-A active site cavity, the shape feature is representative of the shape of the active site.

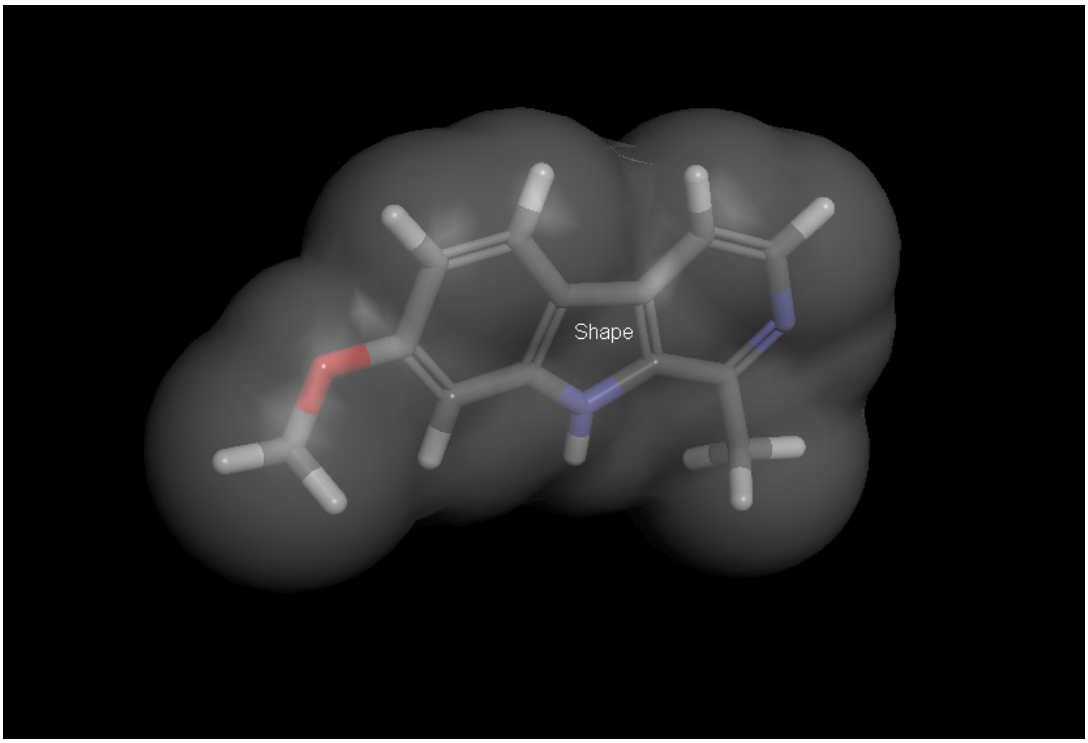

Figure 3.4. Graphical representation of the pharmacophore model derived from the structure of harmine using the *structure-based* approach. In this representation, only the shape feature is illustrated.

To gain insight into the pharmacophore features of the model shown in Fig 3.3, it is helpful to analyze the interactions between the co-crystallized ligand, harmine, and the MAO-A active site. This analysis may be done by displaying the interactions in two-dimensions as well as by calculating the interaction energies between the ligand and individual active site residues and waters. As shown in the two-dimensional representation of these interactions, no π-π interactions exists between harmine and the MAO-A active site. The two-dimensional representation also shows that hydrophobic interactions exist between the ligand and Ile180, Ile335, Gln215 and Phe208. The interaction energies show that these amino acid residues contribute significantly to the total binding energy of the ligand (–2.98, –3.04, –3.81 and –3.35 kcal/mol, respectively). Based on the more negative energies, the interaction with Phe208 and Gln215 is especially important. Additional interactions with Tyr407 and Phe352 are also highlighted in the two-dimensional representation. The two-dimensional representation also indicates that a hydrogen bond exist between an active site water (HOH746) and the endocyclic NH of harmine. For this interaction, the ligand acts as hydrogen bond donor.

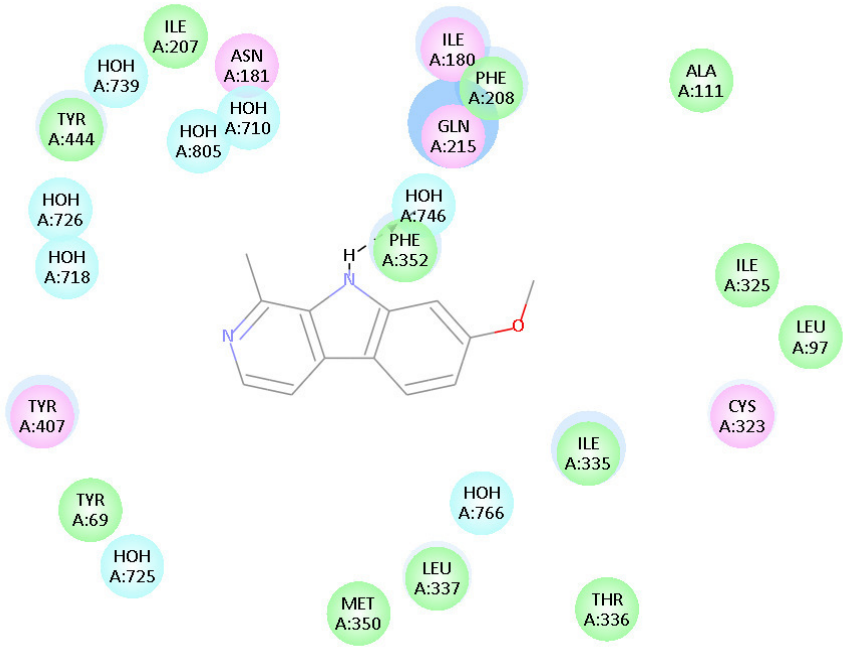

Figure 3.5. A two-dimensional representation of the binding of harmine in the MAO-A active site.

Table 3.1. The interaction energies of harmine with the active site residues and waters of MAO-A. Selected interactions among those that are most productive are shaded.

Name	Forcefield	Total Interaction Energy (kcal/mol)	Total VDW Interaction Energy (kcal/mol)	Total Electrostatic Interaction Energy (kcal/mol)
2Z5X	2Z5X-CHARMm	-35.55529	-33.42394	-2.13135

Interaction Energies			
Residue	**Interaction Energy (kcal/mol)**	**VDW Interaction Energy (kcal/mol)**	**Electrostatic Interaction Energy (kcal/mol)**
A_ALA68	-0.174895	-0.125276	-0.049619
A_TYR69	-1.445820	-1.702340	0.256518
A_LEU97	-0.254956	-0.284683	0.029727
A_PHE108	-0.062479	-0.063678	0.001199
A_ALA111	-0.398734	-0.209775	-0.188959
A_ILE180	-2.978910	-2.962370	-0.016536
A_ASN181	-1.513320	-1.321820	-0.191498
A_TYR197	-0.092397	-0.111140	0.018743

A_ILE207	-0.636574	-0.692979	0.056405
A_PHE208	-3.350520	-3.025380	-0.325139
A_SER209	-0.389800	-0.388625	-0.001175
A_VAL210	-0.554467	-0.590925	0.036458
A_GLN215	-3.810150	-3.874360	0.064214
A_CYS323	-0.804479	-0.665564	-0.138915
A_ILE325	-1.076070	-1.047630	-0.028444
A_ILE335	-3.038290	-3.009070	-0.029220
A_THR336	-0.534294	-0.596513	0.062219
A_LEU337	-1.854170	-1.859750	0.005579
A_MET350	-0.796263	-0.768697	-0.027566
A_PHE352	-1.676600	-1.774460	0.097862
A_TYR407	-2.212980	-2.532430	0.319448
A_TYR444	-0.838804	-0.863405	0.024601
A_FAD600	-2.437070	-1.902470	-0.534595
A_HOH706	-0.241148	-0.119492	-0.121656
A_HOH710	-0.029867	-0.196034	0.166167
A_HOH718	-0.600630	-0.592233	-0.008397
A_HOH725	-0.161973	-0.288885	0.126912
A_HOH726	0.328066	-0.033992	0.362058
A_HOH729	0.008016	-0.046768	0.054784
A_HOH739	-0.324239	-0.431456	0.107217
A_HOH746	-0.451975	0.652085	-1.104060
A_HOH766	-0.956282	-0.953205	-0.003077
A_HOH805	-2.193230	-1.040620	-1.152610

Based on the analysis of the key interactions between the ligand and the MAO-A active site above, the interactions of the ligand with the key residues and waters are shown as a three-dimensional representation in Figure 3.6.

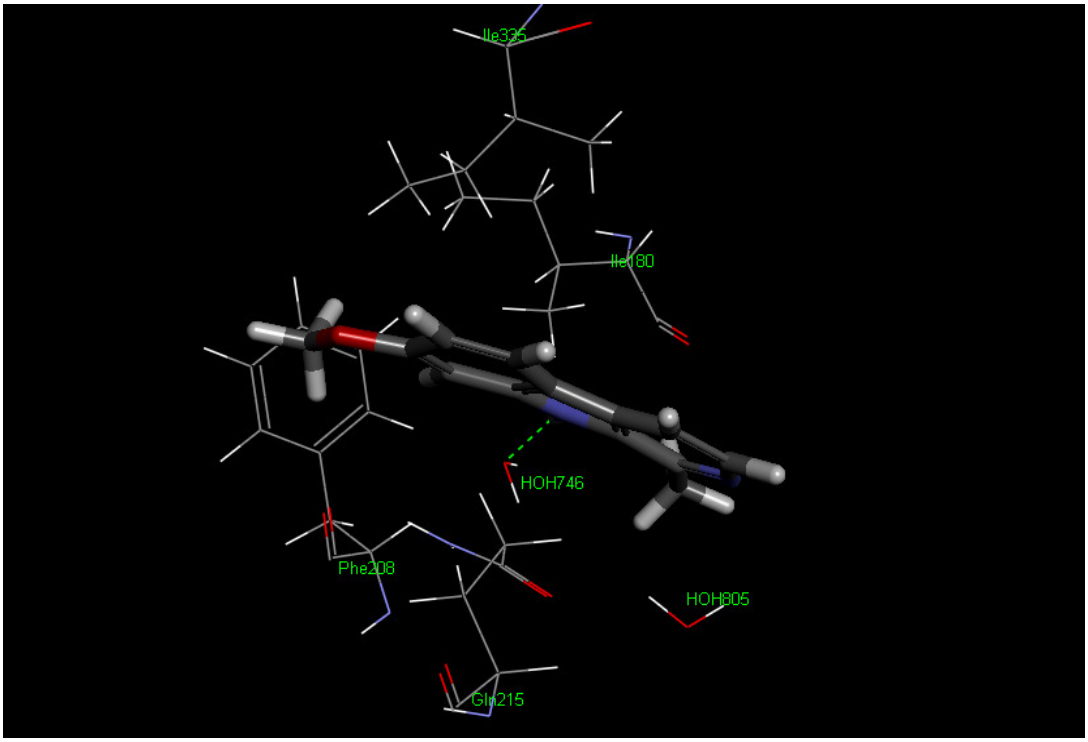

Figure 3.6. A three-dimensional representation of the binding of harmine in the MAO-A active site. The most important interacting residues are also given. Hydrogen bonding is represented by a green dashed line.

As shown in Figure 3.7, the five acceptor features of the pharmacophore model correspond to interactions with the following residues and water molecules:

- Val210, HOH766
- Tyr444
- Gln215
- HOH725
- FAD

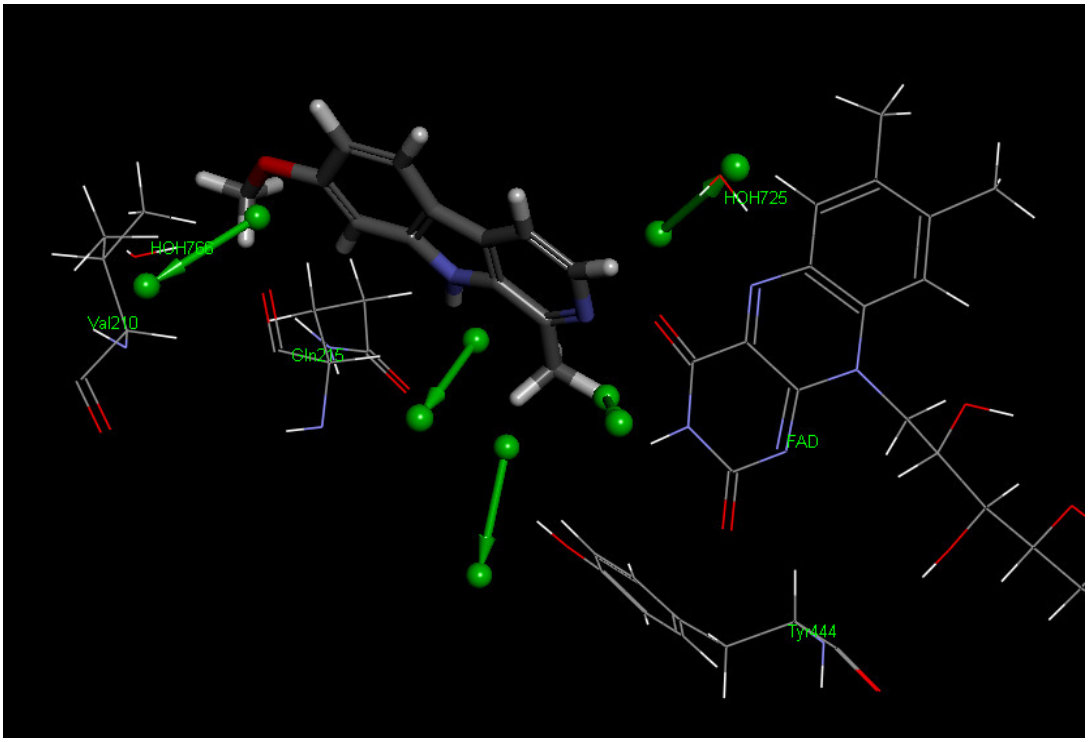

Figure 3.7. A three-dimensional representation of acceptor features and their interacting residues and waters.

As shown in Figure 3.8, the six donor features of the pharmacophore model correspond to interactions with the following residues and water molecule:

- Thr336 (peptide carbonyl)
- Gln215 (side chain amidic carbonyl)
- HOH746
- Phe208 (peptide carbonyl)
- Ans181 (side chain amidic carbonyl)
- Ile180 (peptide carbonyl)

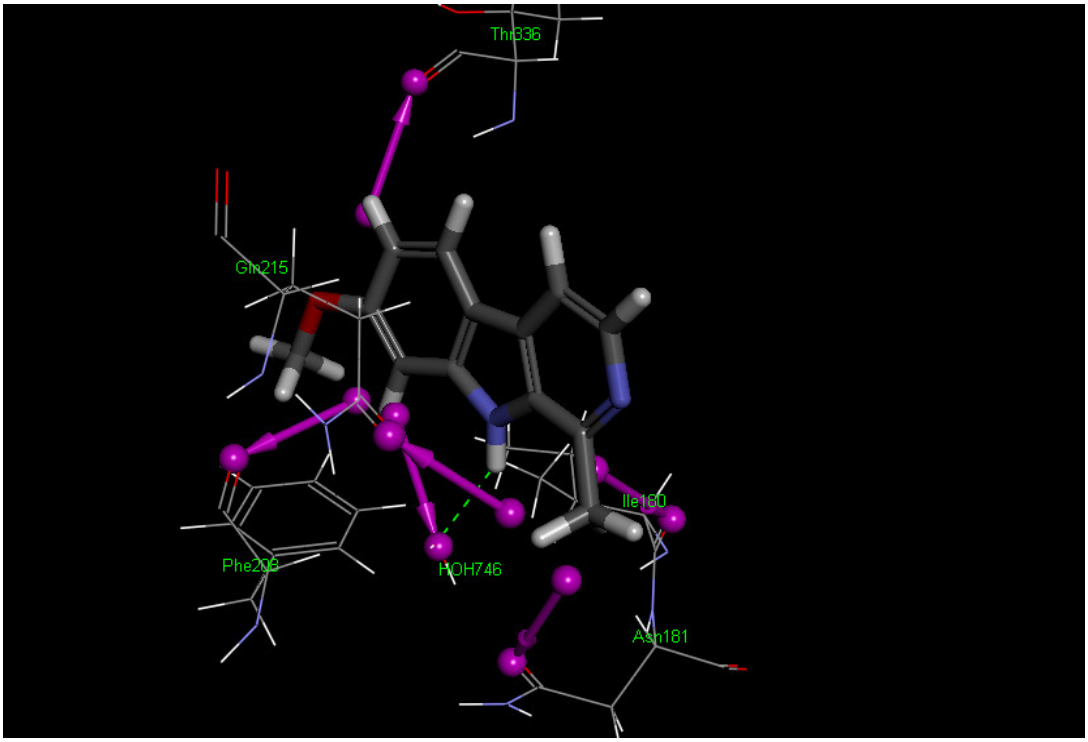

Figure 3.8. A three-dimensional representation of donor features and their interacting residues and water molecule.

The pharmacophore model was subsequently used to screen a virtual library of drug molecules for potential binding to the MAO-A active site. For this purpose, the DrugBank library was used, which contains all of the Food and Drug Administration (FDA) approved drug molecules. A set of conformations was firstly calculated for each molecule in the library. For each compound, 255 conformations were generated using the BEST algorithm of Discovery Studio. These conformations were subsequently mapped to the pharmacophore model using the Screen Library protocol of Discovery Studio. None of the features were set as required features and the fitting method was set to rigid. The drugs that mapped to four pharmacophore features are given in Table 3.2. These represent the hits and were evaluated *in vitro* as inhibitors of recombinant human MAO-A and –B.

Table 3.2. A list of the compounds in the DrugBank which mapped to the pharmacophore model derived from the structure of harmine using the *structure-based* approach. These compounds represent drugs which are used systemically by humans. The shaded entries were found to be four feature hits.

Drug	Structure
Acetaminophen	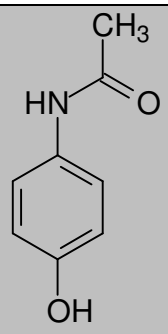
Acyclovir	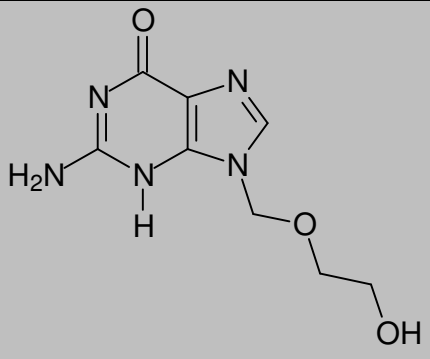
Anagrelide	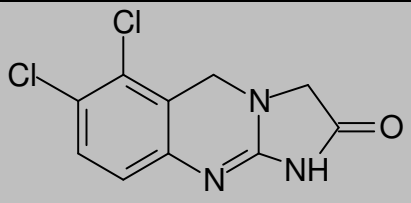
R-(-)-Apomorphine	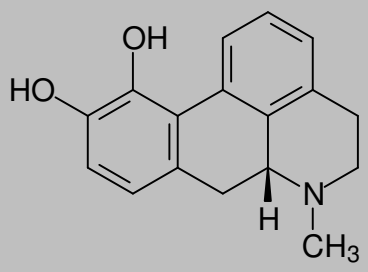

Atenolol	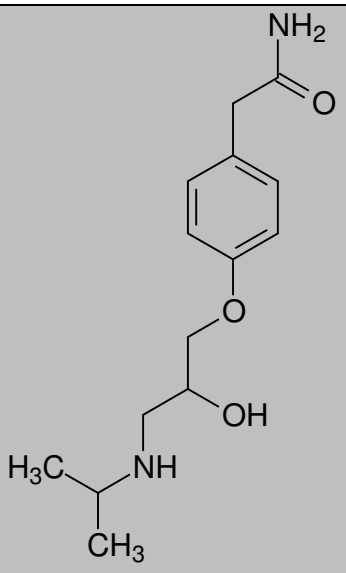
Baclofen	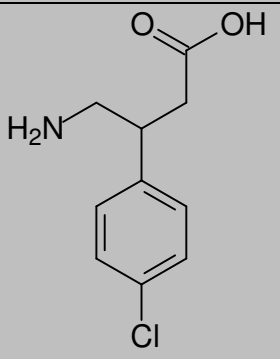
Caffeine	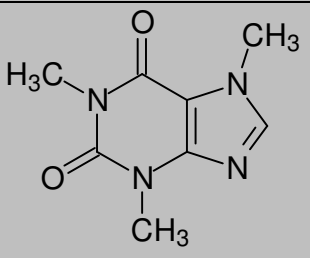

Cladribine	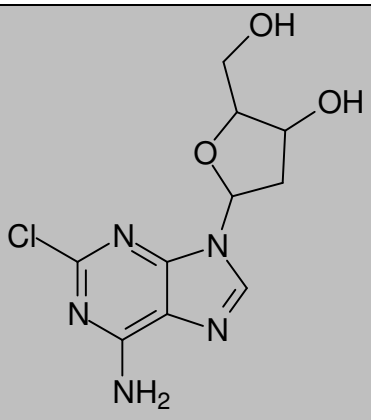
Ethoxzolamide	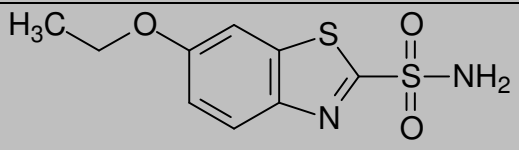
Floxuridine	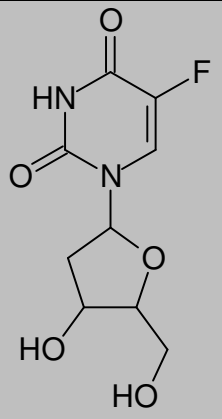
Icosapent	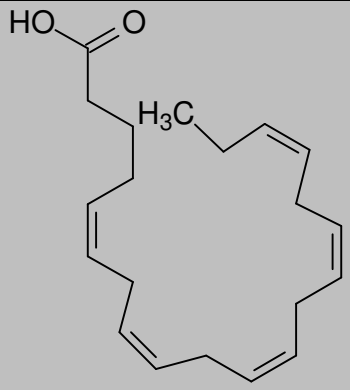

Idoxuridine	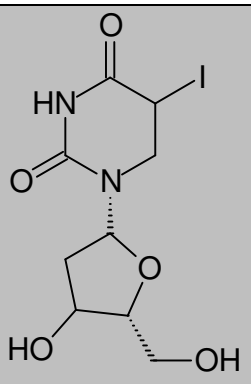
Metformin	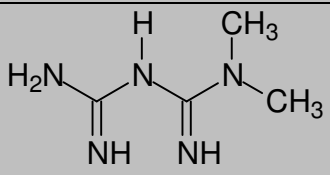
Methyclothiazide	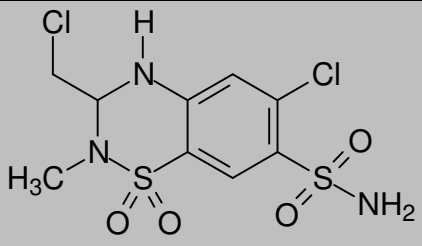
Midodrine	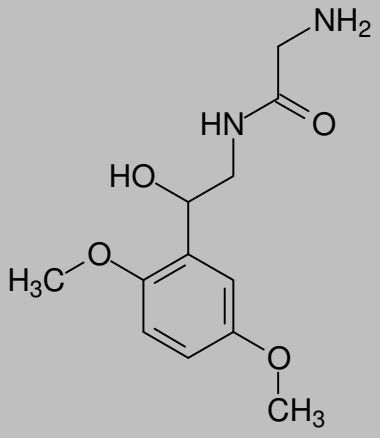

Milrinone	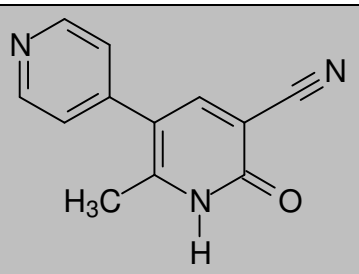
Ondansetron	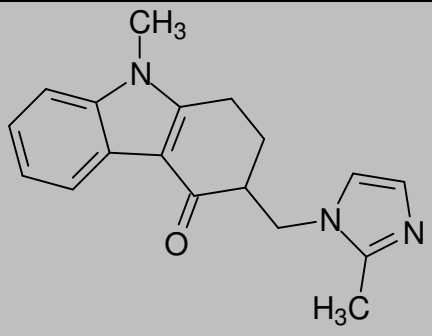
Pipobroman	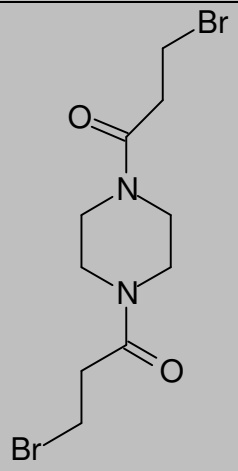
Ropinirole	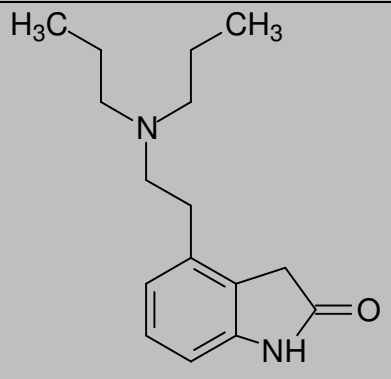

Ropivacaine	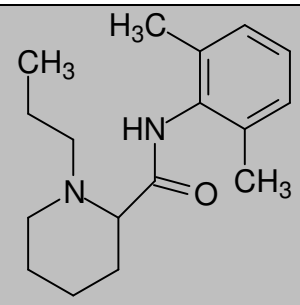
Sulfanilamide	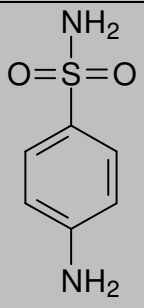
Sulfisoxazole	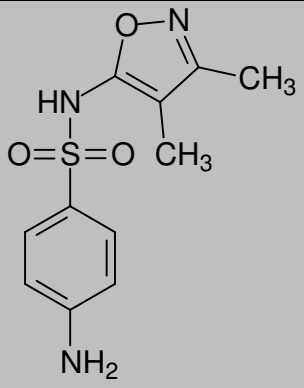
Tolcapone	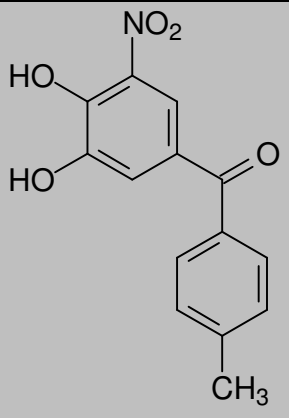

Vidarabine	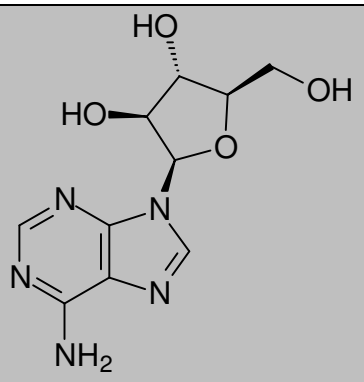

To determine if the pharmacophore model has the ability to also identify known MAO-A inhibitors, a series of 20 test compounds were queried with the pharmacophore model.

Table 3.3. A virtual library of 20 test compounds (11 MAO-A inhibitors and 9 non-inhibitors) was screened with the pharmacophore model. Below is given a list of compounds that were found to be four feature hits. The shaded entries are known MAO-A inhibitors (IC_{50} < 5 μM). The structures, not shaded, are known to not bind to MAO-A. The pharmacophore model used, was derived from the structure of harmine using the *structure-based* approach.

Drug	**Structure**
Amiflamine	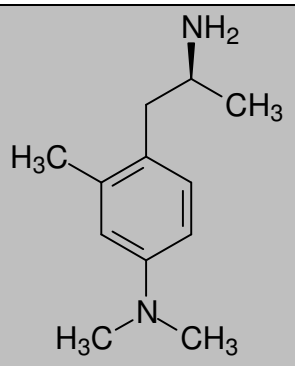

Azure B	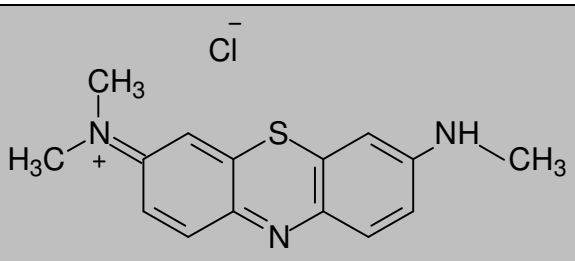
Brofaromine	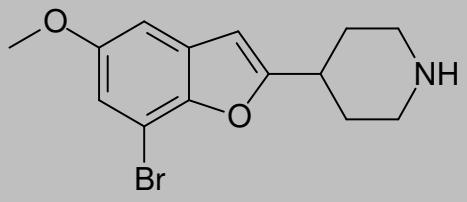
CX157	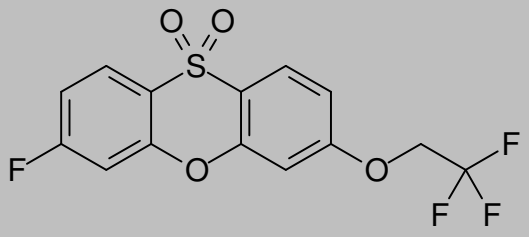
Esuprone	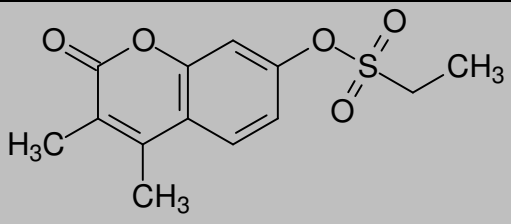
Lazabemide	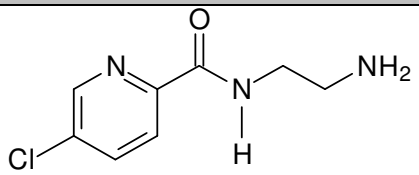
Metralindole	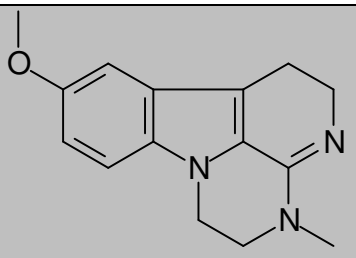

Pirlindole	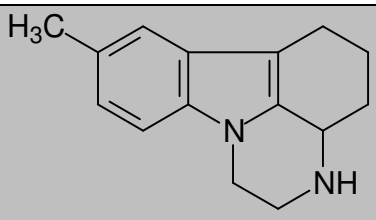
Sercloremine	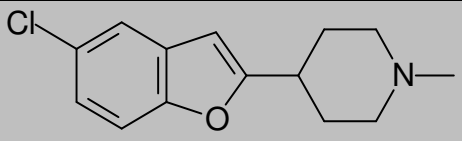
Toloxatone	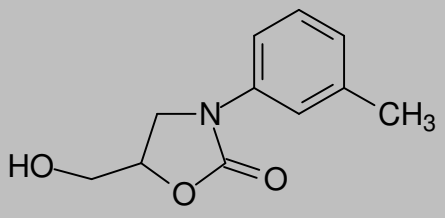

Table 3.4. A virtual library of 20 test compounds (11 MAO-A inhibitors and 9 non-inhibitors) was screened with the pharmacophore model. Below is given a list of compounds that were not four feature hits. The shaded entries are known MAO-A inhibitors (IC_{50} < 5 µM). The structures, not shaded, are known to not bind to MAO-A. The pharmacophore model used, was derived from the structure of harmine using the *structure-based* approach.

Four feature non-hits	
Drug	**Structure**
(E)-8-(3-chlorostyryl)caffeine	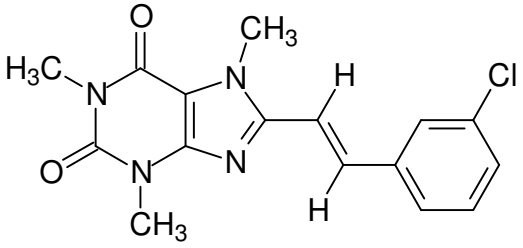

Chromone	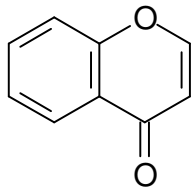
Chromone-3-carboxaldehyde	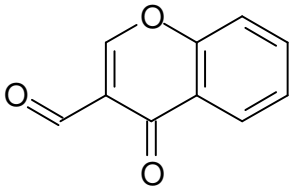
Istradefyline	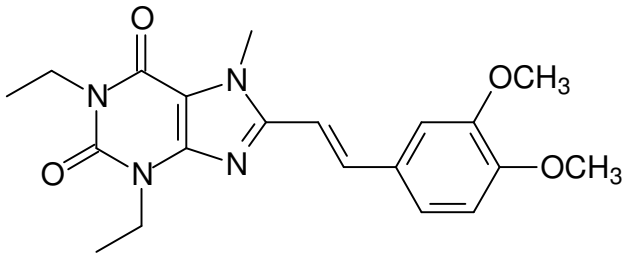
Methylene Blue	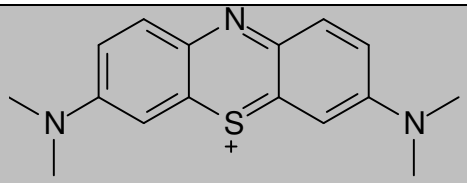
Minaprine	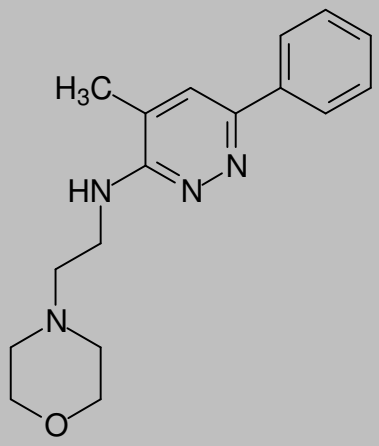

N-Phenylphthalimide	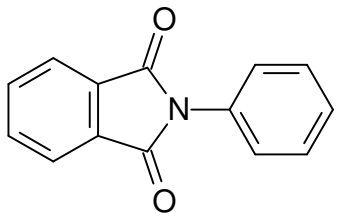
Phthalimide	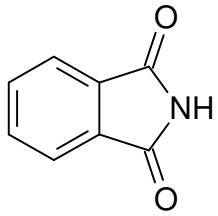
Terbinafine	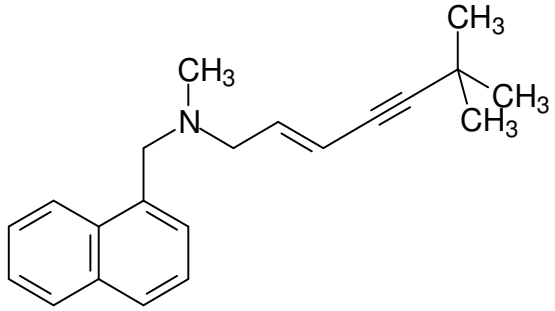
Safinamide	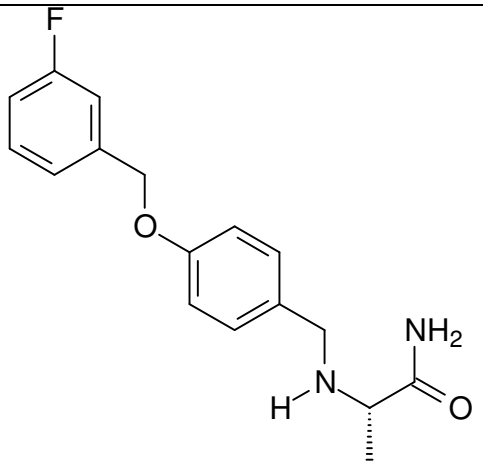

The results shown in tables 3.3 and 3.4 suggest that the model has a reasonable ability to distinguish between known MAO-A inhibitors, and compounds known not to bind to MAO-A. Table 3.3 shows that nine of 11 known MAO-A inhibitors are four feature hits,

while one compound, lazabemide, which is not a MAO-A inhibitor was also found to map to the pharmacophore. Table 3.4 shows that eight non-inhibitors from an evaluated nine were not hits, while two known MAO-A inhibitors were found not to be hits with the pharmacophore model. These results suggest that the pharmacophore model may be suitable for the screening of a virtual library for compounds with affinities for MAO-A.

3.3.2. Structure-based pharmacophore of MAO-B

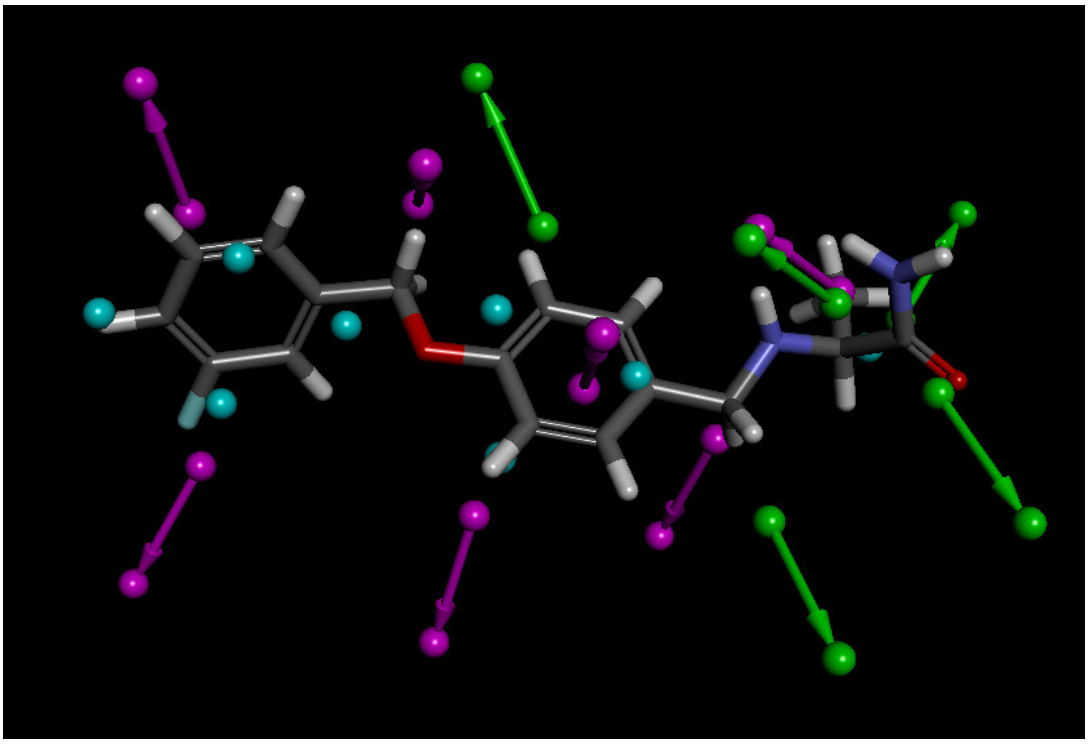

Figure 3.9. Graphical representation of the pharmacophore model derived from the structure of safinamide using the *structure-based* approach. This model may be used to screen a virtual library for structures that bind to MAO-B. The green arrows represent hydrogen bond acceptor features, the purple arrows represent hydrogen bond donor features and the cyan spheres represent hydrophobic features.

For the construction of this pharmacophore model (Fig. 3.9), the X-ray crystal structure of human MAO-B with safinamide co-crystallized in the active site was used (PDB code: 2V5Z). All calculations were carried out with Discovery Studio 3.1. The software firstly calculated the interactions between safinamide and the amino acid residues and water

molecules of the active site. The software also determines additional interactions which may exist between a ligand and the MAO-B active site. Based on these possible interactions, pharmacophore features are placed in the active site. These features are hydrogen bond acceptor features, hydrogen bond donor features and hydrophobic features. The user then allows the software to cluster the feature groups. In this way a group of features that represents the same interactions are grouped into a single feature. Location constraints are subsequently added to each feature. These are spheres which are placed around the features (at center) and define the ideal location for the ligand atom(s). The sphere represents the tolerance of the allowable deviation of the ligand atom(s) from the ideal position. In the last step, a shape feature is placed around safinamide (Fig. 3.10). When searching a virtual database for ligands that may map to the pharmacophore model, the algorithm attempts to fill up the shape, not just have the structure fit inside it. Since safinamide is a relatively large inhibitor and fills the MAO-B active site cavity, the shape feature is representative of the shape of the active site.

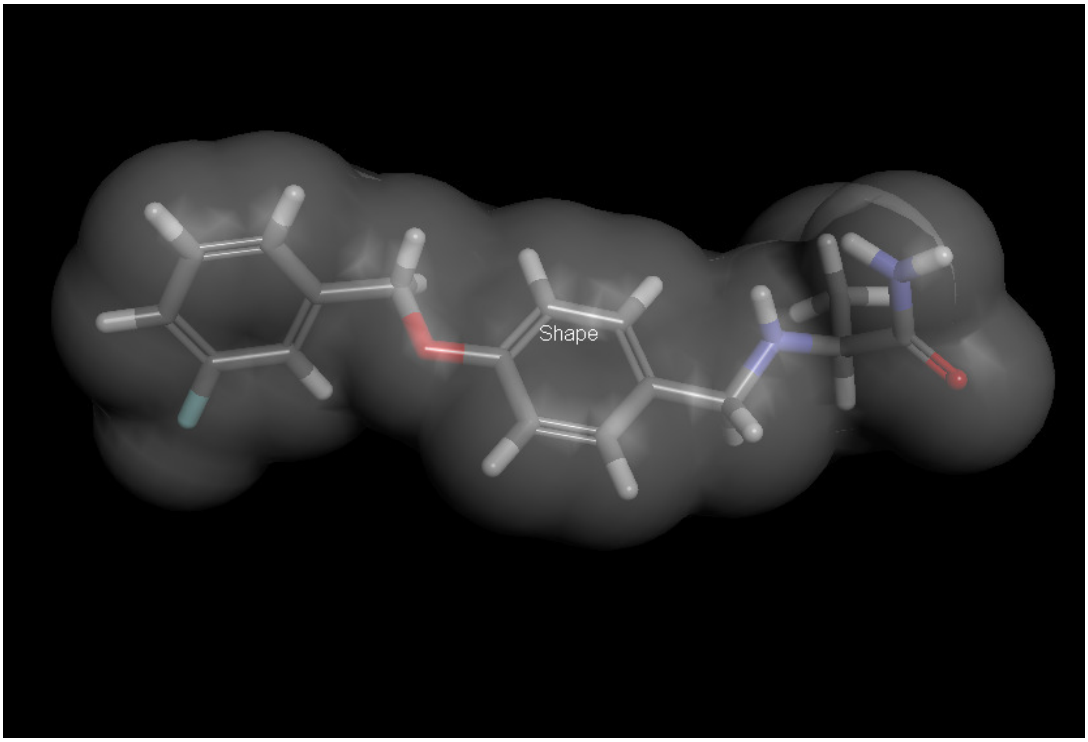

Figure 3.10. Graphical representation of the pharmacophore model derived from the structure of safinamide using the *structure-based* approach. In this representation, only the shape feature is illustrated.

To gain insight into the pharmacophore features of the model shown in Fig 3.9, it is useful to analyze the interactions of the co-crystallized ligand, safinamide, with the active site of MAO-B. This analysis may be done by displaying the interactions in two-dimensions as well as by calculating the interaction energies between the ligand and individual active site residues and waters. As shown in the two-dimensional representation of these interactions, no π-π interactions exists between safinamide and the MAO-B active site. The two-dimensional representation also shows that hydrophobic interactions exist between the ligand and Leu171, Ile199, Gln206 and Ile316. The interaction energies show that these amino acid residues contribute significantly to the total binding energy of the ligand (–4.46, –5.93, –5.54 and –2.09 kcal/mol, respectively). Based on the more negative energies, the interaction with Ile199 and Gln206 is especially important. As discussed below, much of the stabilization afforded by Gln206 is due to hydrogen bonding. The two-dimensional representation

also indicates that a hydrogen bond exist between an active site water (HOH1351) and the amide carbonyl oxygen of the ligand. For this interaction, the ligand acts as hydrogen bond acceptor. This interaction contributes significantly to the stabilization of the ligand (–1.94 kcal/mol). Furthermore, two hydrogen bonds are formed between the amide NH_2 and side chain NH and the side chain carbonyl oxygen of Gln206. For both these interactions, the ligand acts as hydrogen bond donor. These interactions may contribute to the stabilization of the ligand by Gln206 (Electrostatic interaction of –2.26 kcal/mol). As shown in the figure, hydrogen bonding between the amide NH_2 and HOH1169 also occurs.

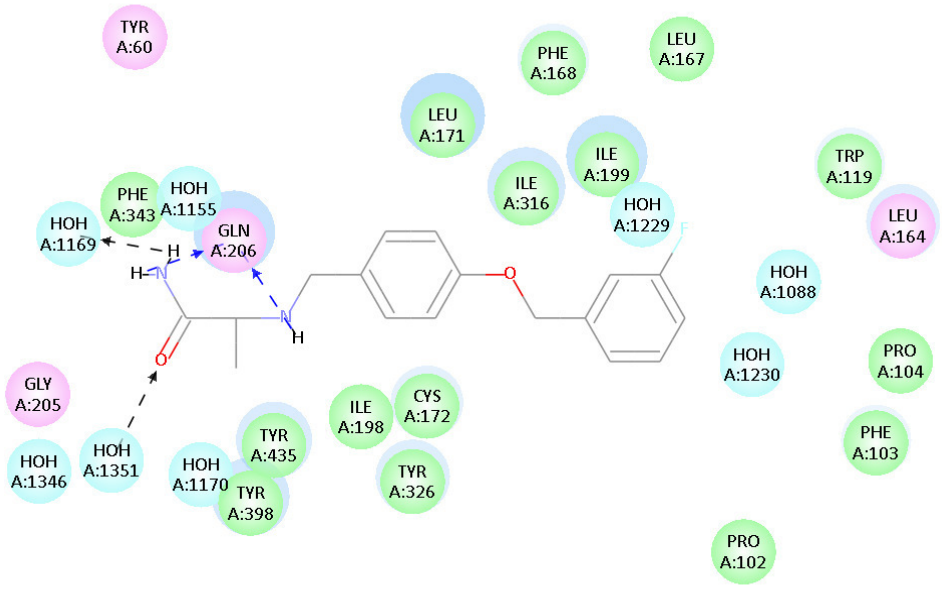

Figure 3.11. A two-dimensional representation of the binding of safinamide in the MAO-B active site.

Table 3.5. The interaction energies of safinamide with the active site residues and waters of MAO-B. Selected interactions among those that are most productive are shaded.

Name	Forcefield	Total Interaction Energy (kcal/mol)	Total VDW Interaction Energy (kcal/mol)	Total Electrostatic Interaction Energy (kcal/mol)
2V5Z	2V5Z-CHARMm	-54.93490	-49.41938	-5.51552

Interaction Energies			
Residue	**Interaction Energy (kcal/mol)**	**VDW Interaction Energy (kcal/mol)**	**Electrostatic Interaction Energy (kcal/mol)**
A_SER59	-0.116731	-0.165970	0.049239
A_TYR60	-1.749280	-1.942620	0.193344
A_VAL61	-0.129577	-0.100429	-0.029148
A_GLN65	-0.066627	-0.078536	0.011909
A_PHE99	-0.160099	-0.185575	0.025476
A_PRO102	-1.096920	-0.661497	-0.435423
A_PHE103	-1.347500	-1.344750	-0.002751
A_PRO104	-0.971124	-1.020070	0.048946
A_TRP119	-1.387880	-1.332350	-0.055529
A_LEU164	-1.320870	-1.613900	0.293033
A_LEU167	-1.181250	-1.111380	-0.069874
A_PHE168	-2.413960	-2.257700	-0.156256
A_LEU171	-4.462220	-4.421540	-0.040684
A_CYS172	-1.692370	-1.583250	-0.109118
A_ILE198	-2.258510	-2.310550	0.052040
A_ILE199	-5.931470	-5.486430	-0.445043
A_SER200	-0.501759	-0.387485	-0.114274
A_GLY205	-0.642355	-0.526771	-0.115584
A_GLN206	-5.537610	-3.274520	-2.263090
A_LYS296	-0.022400	-0.091742	0.069342
A_ILE316	-2.091010	-2.080920	-0.010086
A_TYR326	-3.409500	-2.816930	-0.592567
A_LEU328	-0.227268	-0.297972	0.070704
A_MET341	-0.116127	-0.138511	0.022384
A_PHE343	-1.202570	-1.160340	-0.042227
A_TYR398	-2.956220	-2.965950	0.009726
A_TYR435	-1.753810	-1.663060	-0.090746
A_FAD1502	-4.852120	-3.675600	-1.176520

A_HOH1088	-0.126392	-0.610260	0.483868
A_HOH1091	-0.007214	-0.049326	0.042112
A_HOH1155	-0.413698	-0.301429	-0.112269
A_HOH1169	-0.312573	-0.416335	0.103762
A_HOH1170	-1.409370	-1.676880	0.267511
A_HOH1229	-0.316147	-0.621550	0.305403
A_HOH1230	-0.499815	-0.223145	-0.276670
A_HOH1346	-0.315002	-0.540869	0.225867
A_HOH1351	-1.935550	-0.283220	-1.652330

Based on the analysis of the key interactions between the ligand and the MAO-B active site above, the interactions of the ligand with the key residues and waters are shown as a three-dimensional representation in Figure 3.12.

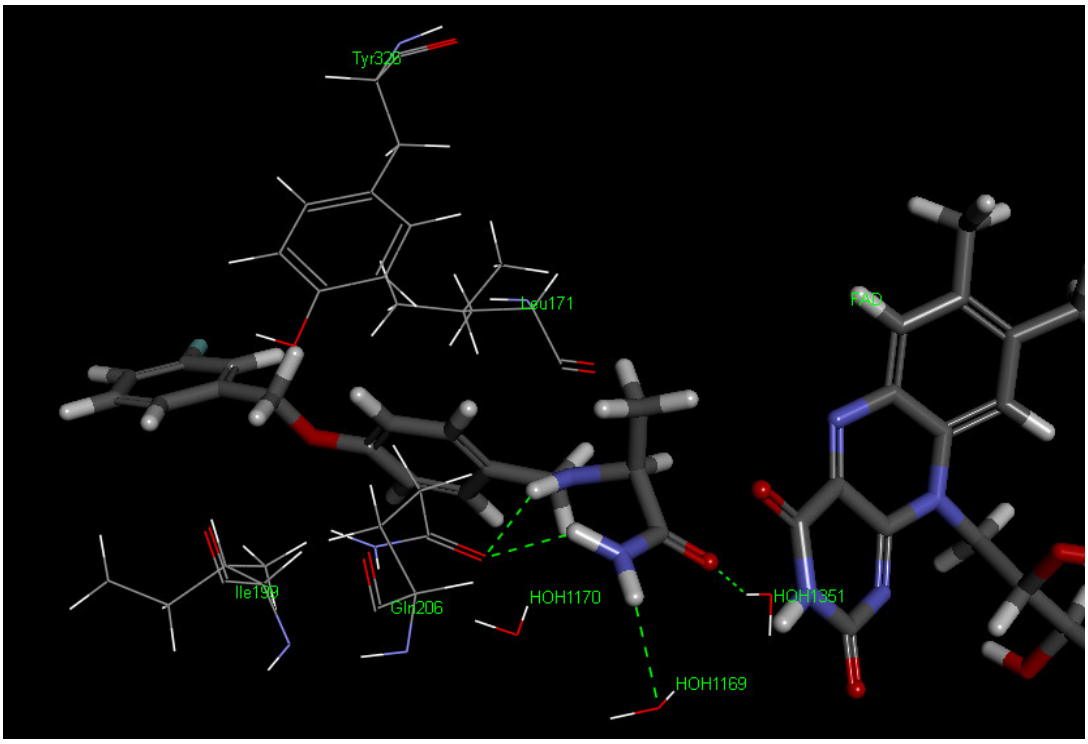

Figure 3.12. A three-dimensional representation of the binding of safinamide in the MAO-B active site. The most important interacting residues are also given. The hydrogen bonding is shown as a green dashed line.

As shown in Figure 3.13, the five acceptor features of the pharmacophore model correspond to interactions with the following residues and water molecules:

- Tyr326, HOH1229 and HOH1230
- HOH1351
- Gln206
- HOH1155
- Lys296 and HOH1346

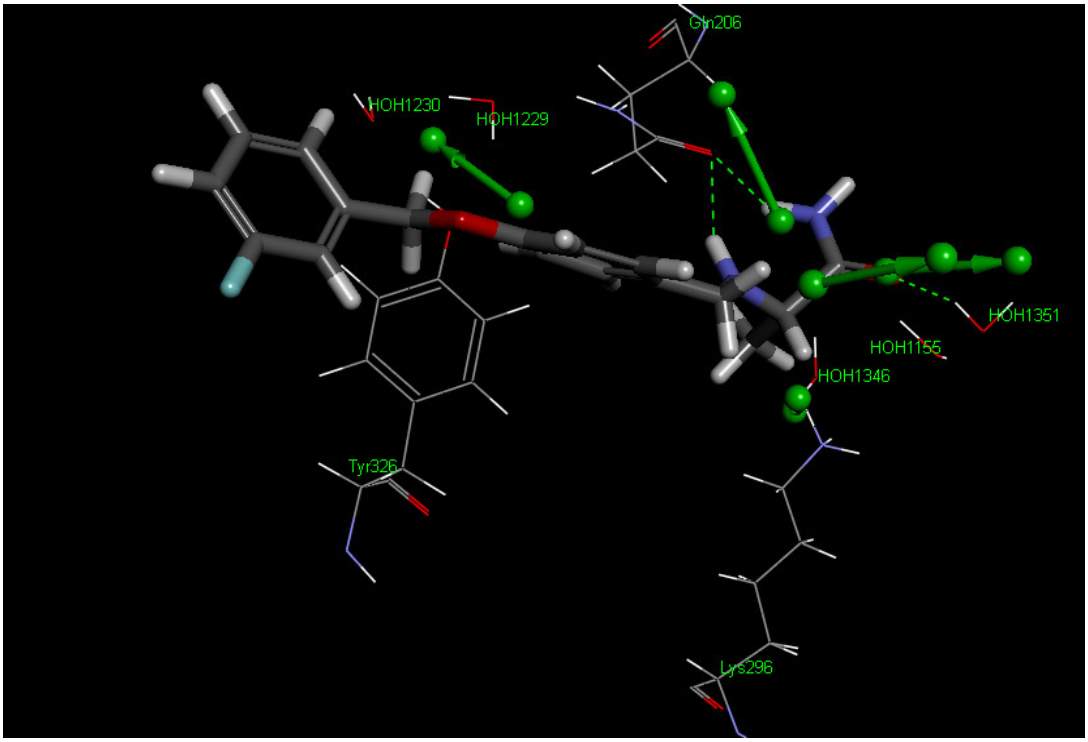

Figure 3.13. A three-dimensional representation of acceptor features and their interacting residues and waters.

As shown in Figure 3.14, the seven donor features of the pharmacophore model correspond to interactions with the following residues:

- Pro102 (peptide carbonyl)
- Ile199 (peptide carbonyl)
- Ile198 (peptide carbonyl)
- Gln206 (side chain amidic carbonyl)
- Leu171 (peptide carbonyl)
- Phe168 (peptide carbonyl)
- Leu164 (peptide carbonyl)

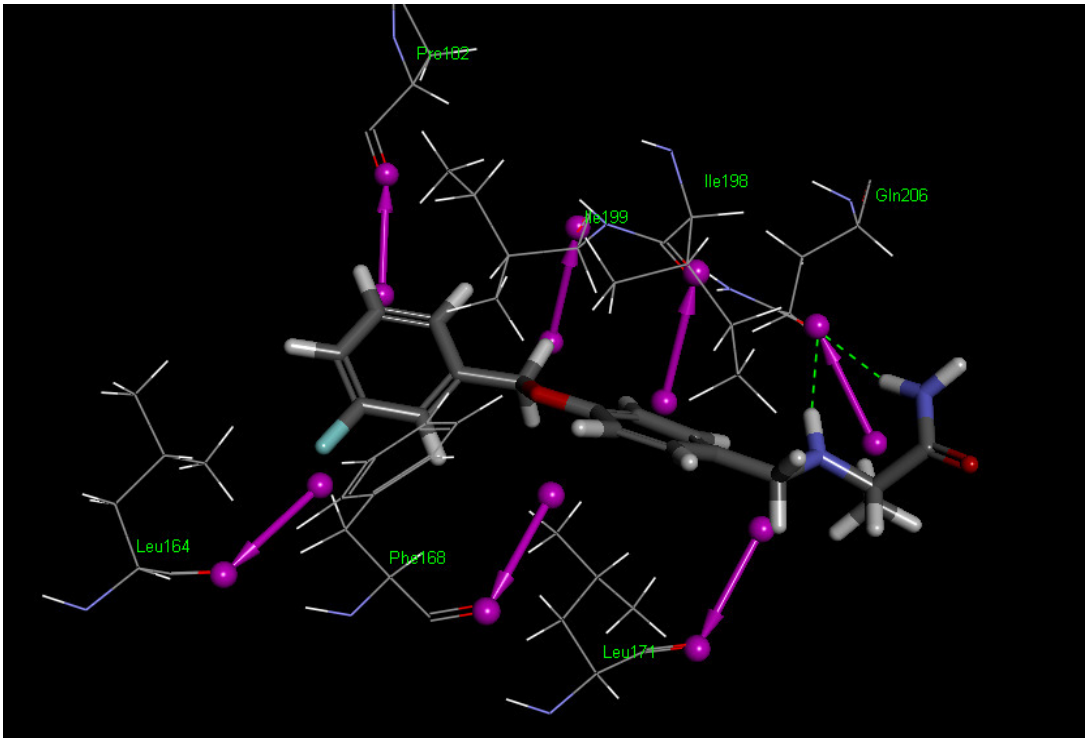

Figure 3.14. A three-dimensional representation of donor features and their interacting residues and water molecule.

The pharmacophore model was subsequently used to screen a virtual library of drug molecules for potential binding to the MAO-B active site. For this purpose, the DrugBank library was used, which contains all of the FDA approved drug molecules. A

set of conformations was firstly calculated for each molecule in the library. For each compound, 255 conformations were generated using the BEST algorithm of Discovery Studio. These conformations were subsequently mapped to the pharmacophore model using the Screen Library protocol of Discovery Studio. None of the features were set as required features and the fitting method was set to rigid. The drugs that mapped to four pharmacophore features are given in Table 3.6. These represent the hits and were evaluated *in vitro* as inhibitors of recombinant human MAO-A and –B. The shaded entries were found to be four features hits.

Table 3.6. A list of the compounds in the DrugBank which mapped to the pharmacophore model derived from the structure of safinamide using the *structure-based* approach. These compounds represent drugs which are used systemically by humans. The shaded entries were found to be four feature hits.

Drug	Structure
Betaxolol	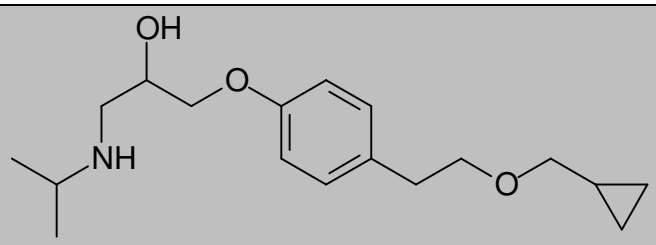
Calcidiol	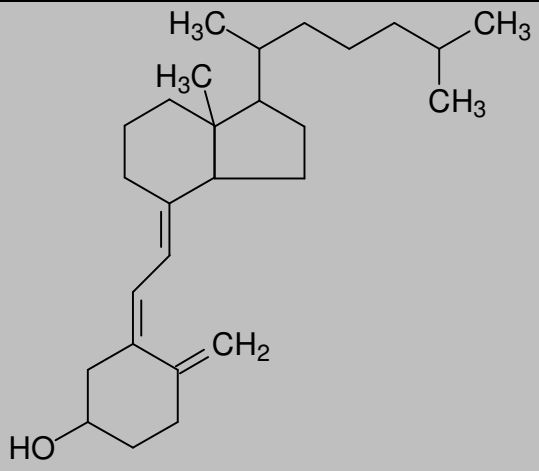

Cholecalciferol	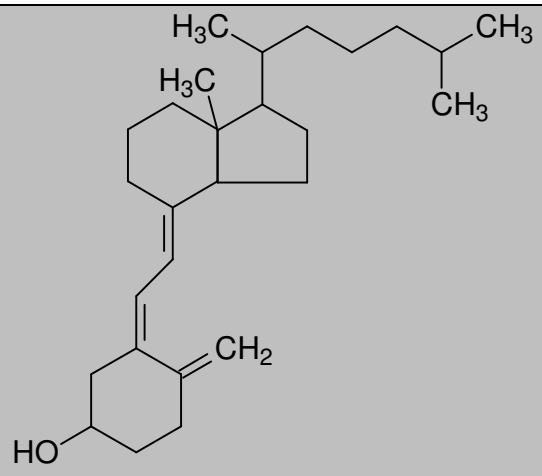
Dantroline	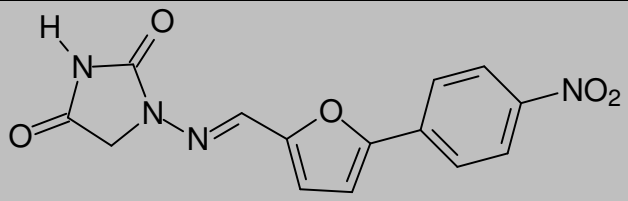
Eletriptan	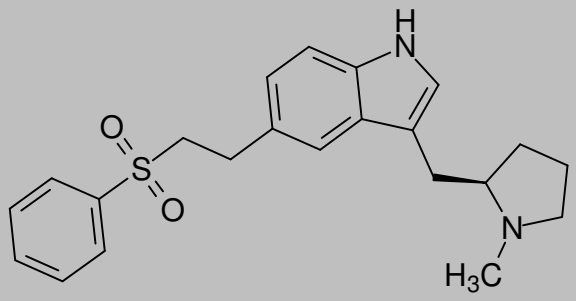

Ergocalciferol	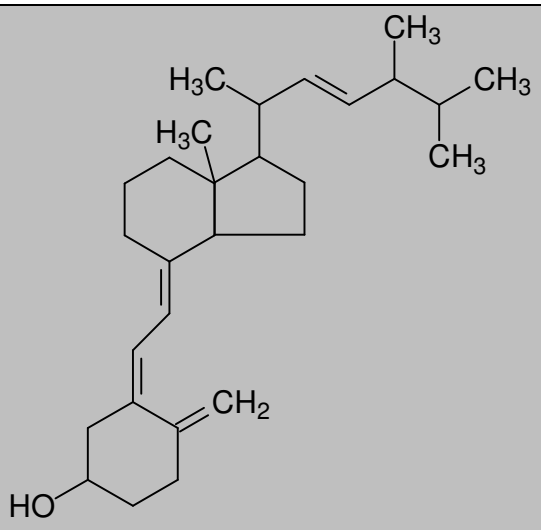
Esmolol	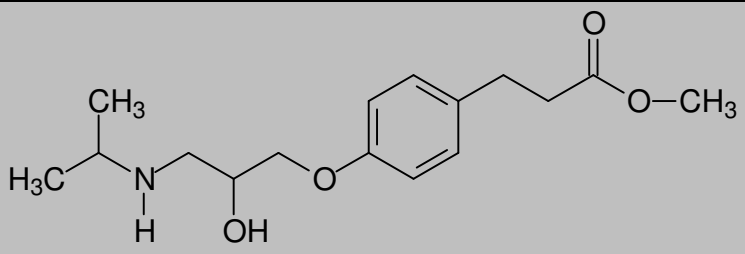
Esomeprazole	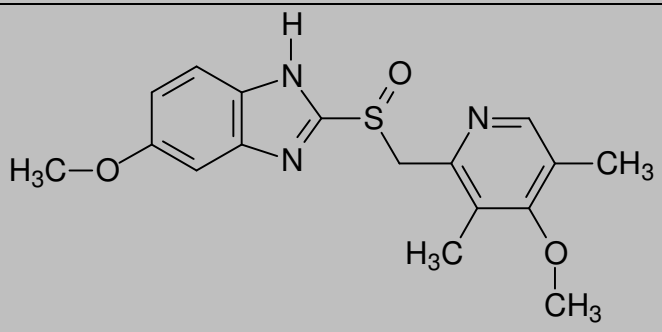
Ethambutol	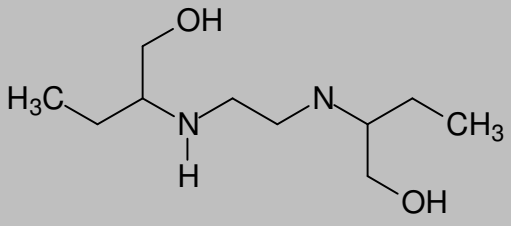

Flurbiprofen	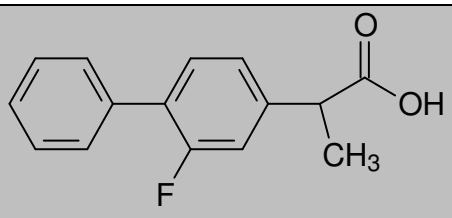
Fluvoxamine	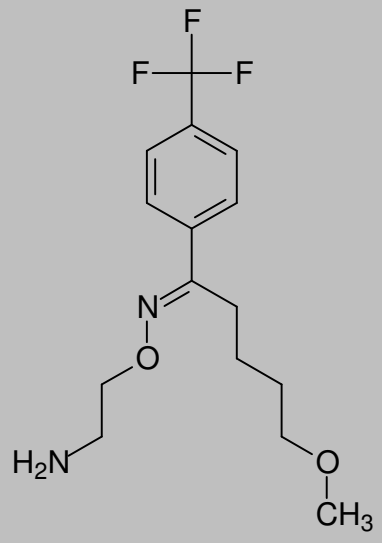
Hesperetin	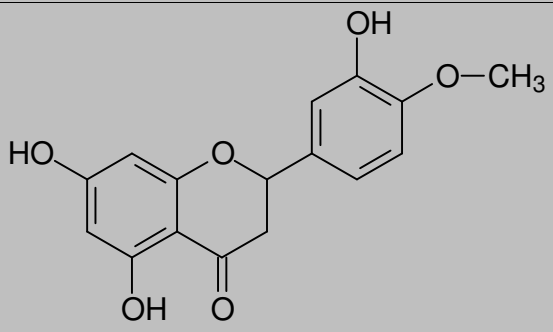

Leflunomide	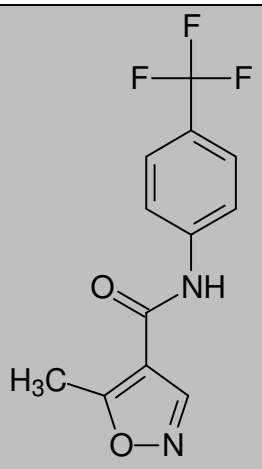
Masoprocol	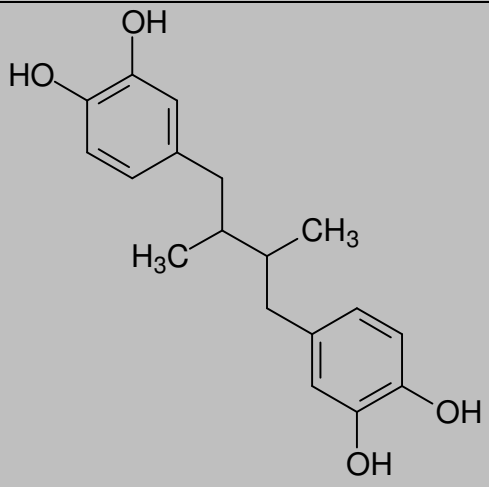
Midodrine	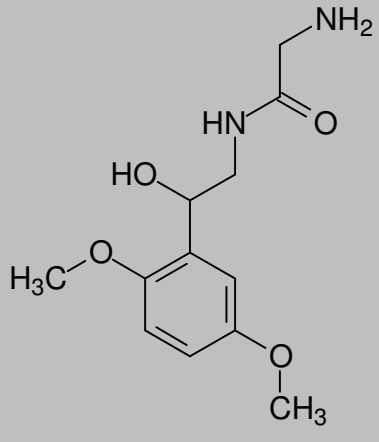

Minaprine	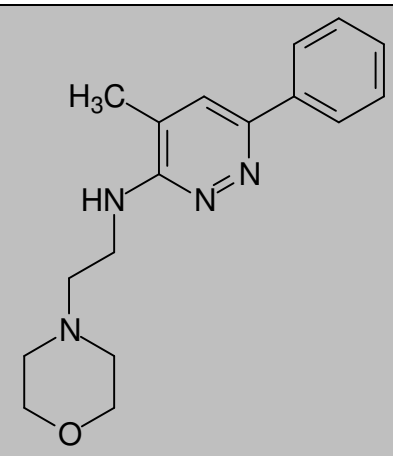
Naproxen	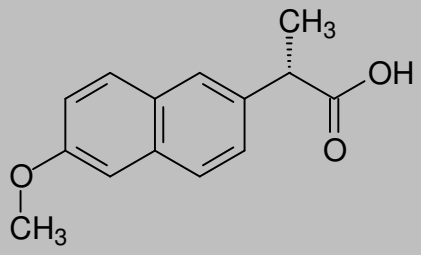
Pantoprazole	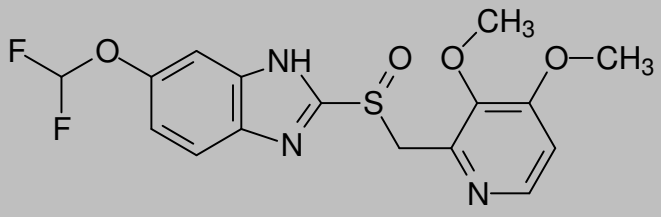
Propranolol	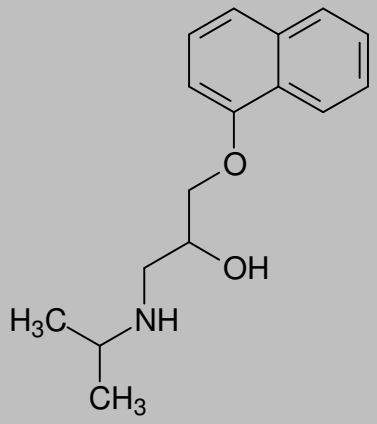

Ramipril	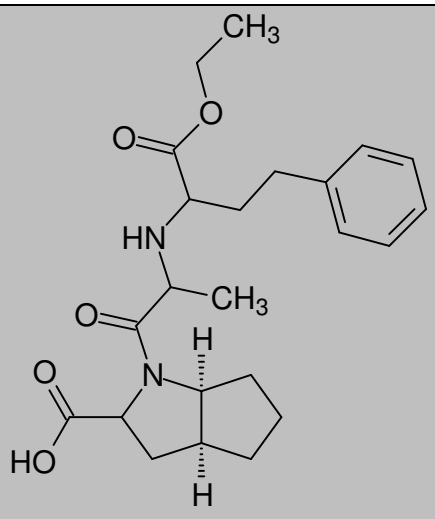
Ritodrine	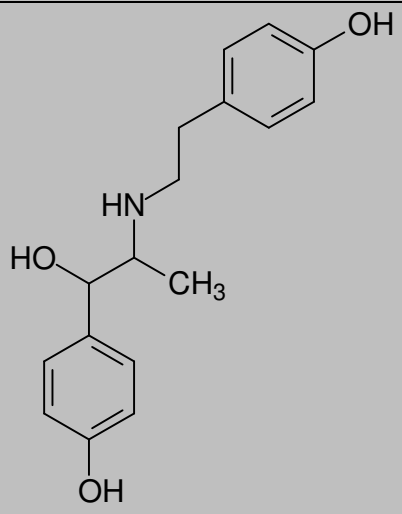
Tolmetin	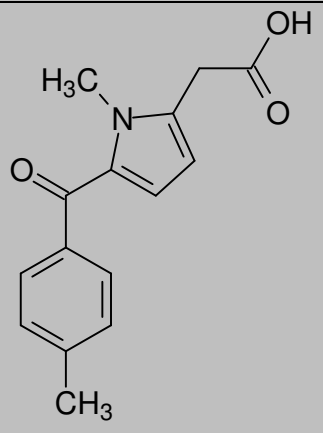

Tolnaftate	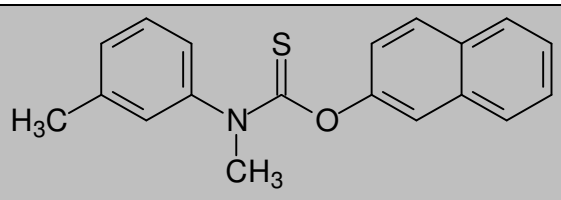
Torasemide	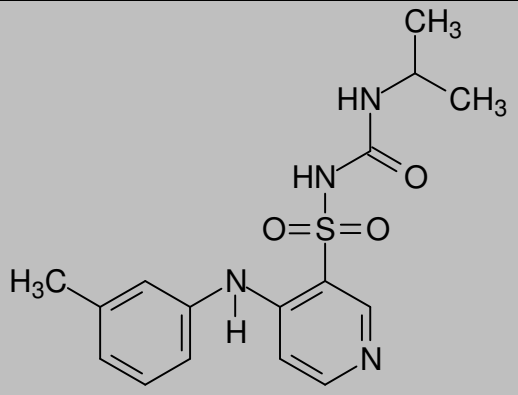
Tramadol	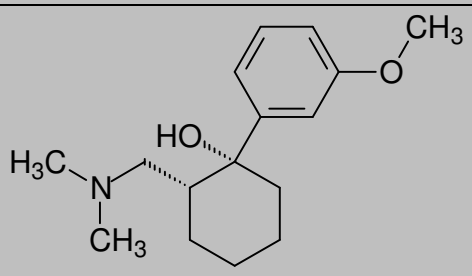

Table 3.7. A virtual library of 30 test compounds (20 MAO-B inhibitors and 10 non-inhibitors) was screened with the pharmacophore model. Below is given a list of compounds that were found to be four feature hits. The shaded entries are known MAO-B inhibitors (IC_{50} < 5 μM). The structures, not shaded, are known to not bind to MAO-B. The pharmacophore model used was derived from the structure of safinamide using the *structure-based* approach.

Drug	Structure
BS 1b	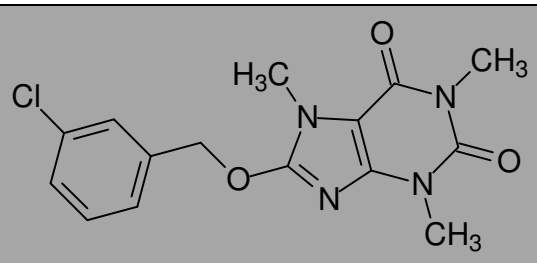
BS 2i	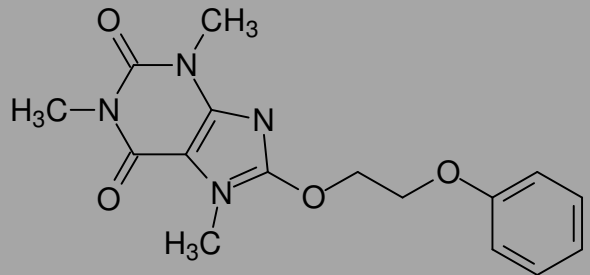
BS 2k	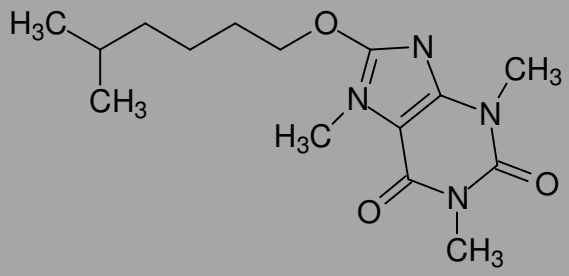

BS 3e	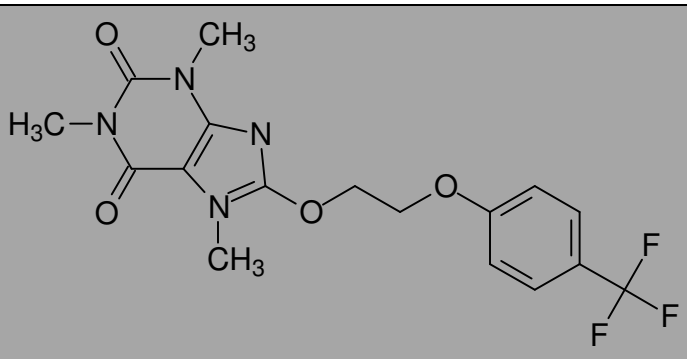
CMK 1i	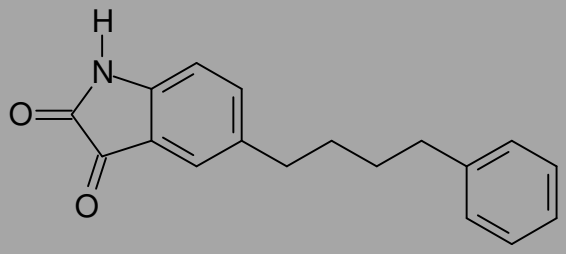
CMK 2g	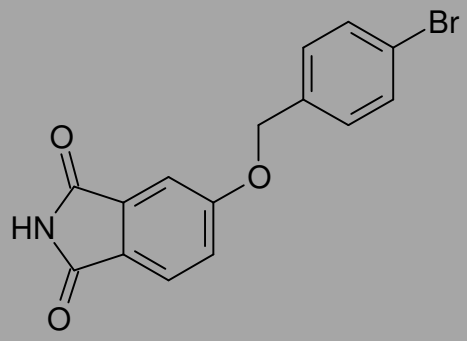
CMK 4h	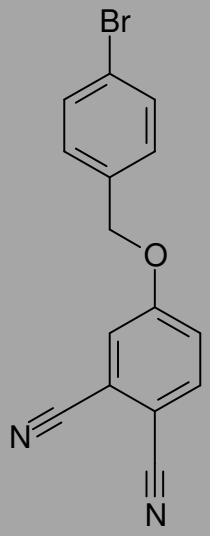

CMK 5f	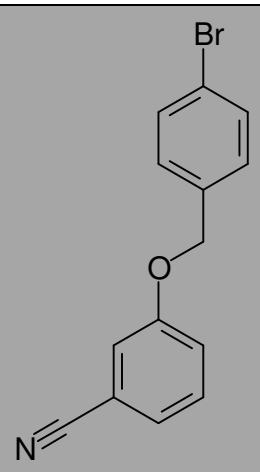
HK 2c	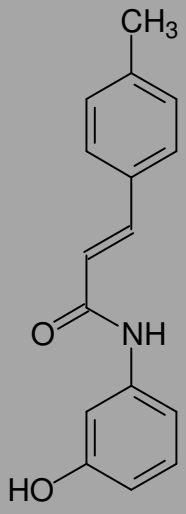
HK 2d	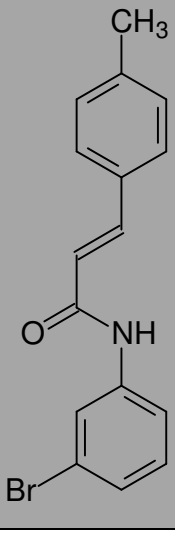

LL 1a	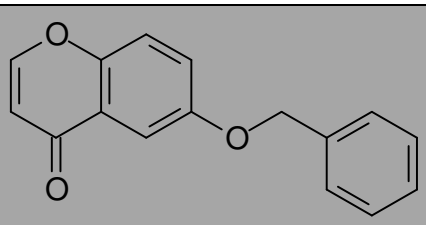
LL 2e	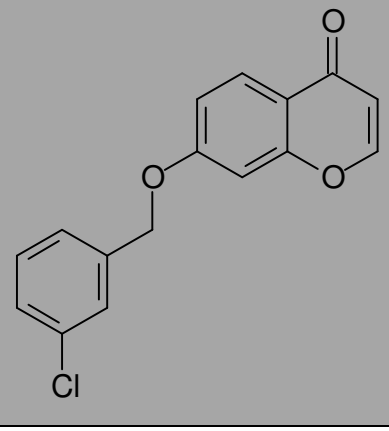
Naproxen	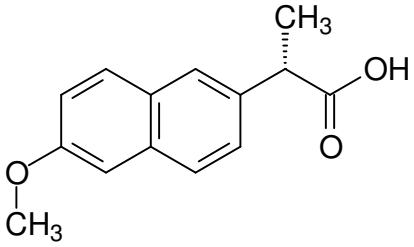
PB 1f	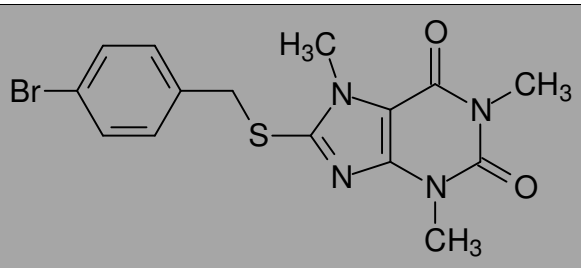
SM 02	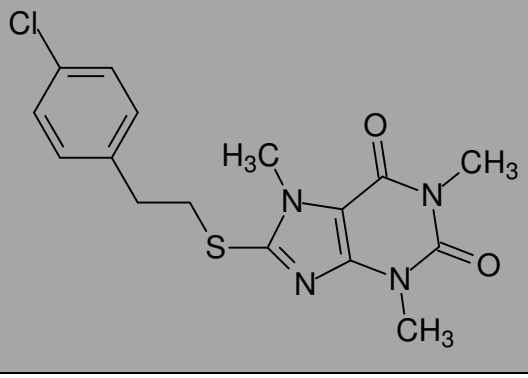

Safinamide	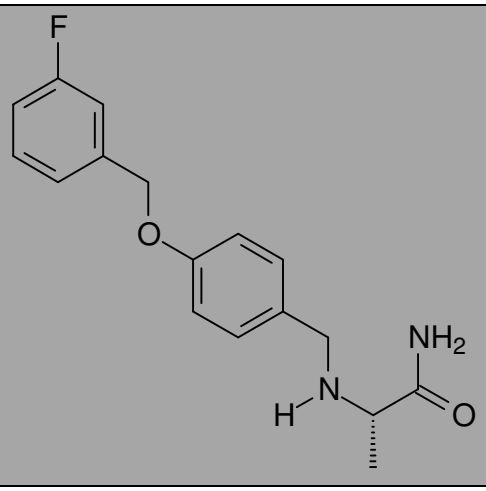
Terbinafine	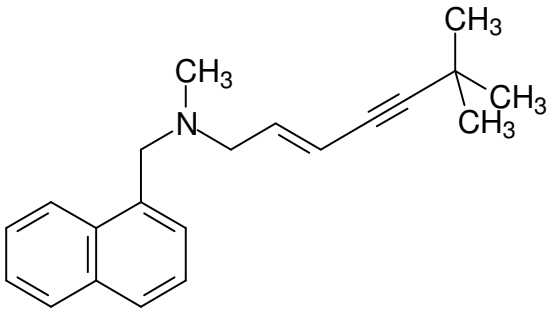
Tolmetin	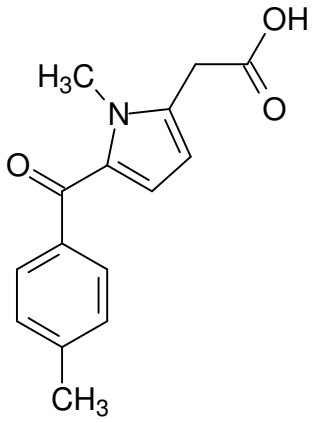

Table 3.8. A virtual library of 30 test compounds (20 MAO-B inhibitors and 10 non-inhibitors) was screened with the pharmacophore model. Below is given a list of compounds that were not four feature hits. The shaded entries are known MAO-B inhibitors (IC_{50} < 5 µM). The structures, not shaded, are known to not bind to MAO-B. The pharmacophore model used, was derived from the structure of safinamide using the *structure-based* approach.

Four feature non-hits	
Drug	**Structure**
Caffeine	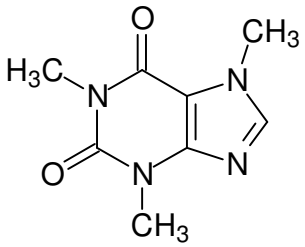
Chromone	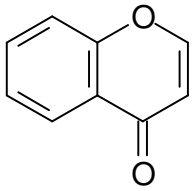
Chromone-3-carboxaldehyde	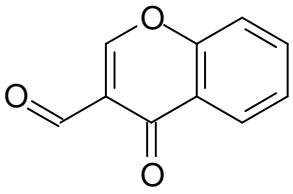
CMK 1k	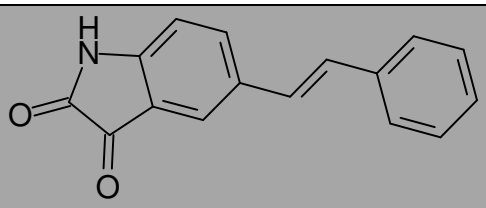

CSC	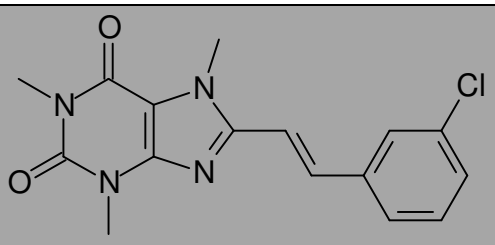
Flurbiprofen	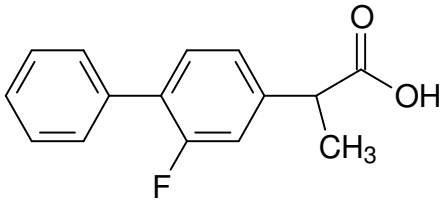
Istradefyline	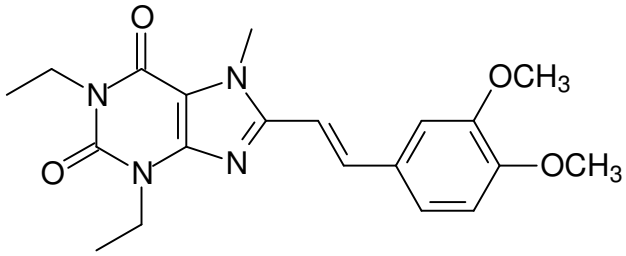
Lazabemide	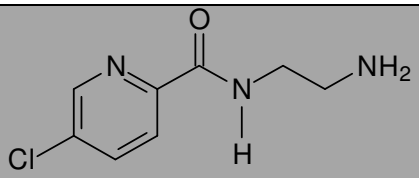
LL 1e	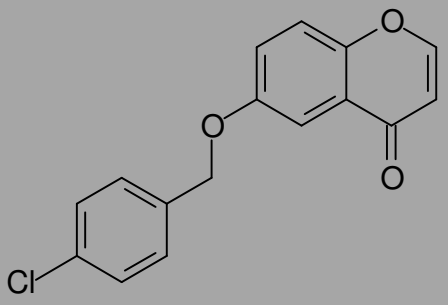

LL 2a	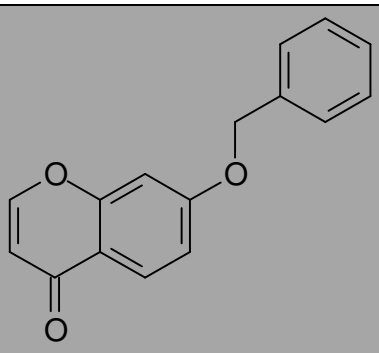
N-Phenylphthalimide	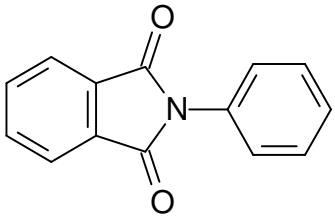
Phthalimide	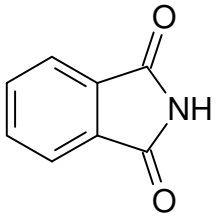

Tables 3.7 and 3.8 show that the MAO-B pharmacophore model possesses a reasonable ability to distinguish between known MAO-B inhibitors, and structures known not to bind to MAO-B. The results in table 3.7 show that 15 from a possible 20 known MAO-B inhibitors are four feature hits. Three of an evaluated total of 10 compounds known not to bind to MAO-B were also found to be hits. Table 3.8 shows that seven non-inhibitors from an evaluated ten were not hits, while five known MAO-B inhibitors were found not to be hits with the pharmacophore model. These results suggest that the pharmacophore model may be suitable for the screening of a virtual library for compounds with affinities for MAO-B. Since three non-inhibitors were also hits, it may be expected that the model could also map non-inhibitors to the model and therefore return false hits. Also, five known inhibitors did not map to the pharmacophore which indicates that not all MAO-B inhibitors in a virtual library will be hits.

3.4. Summary

This chapter describes how structure-based pharmacophore models of MAO-A and MAO-B may be constructed. It is also shown that these models possess reasonable abilities to distinguish between known inhibitors and compounds known not to inhibit. Using these models, the DrugBank library of FDA approved drugs was screened for compounds with potential binding to MAO-A and MAO-B. Among the hits, 29 compounds were selected for evaluation as MAO-A and MAO-B inhibitors. These compounds are listed below. Their inhibitory potencies towards MAO-A and MAO-B will be presented in Chapter 4. In addition, the docked orientations and interactions of selected drugs which are found to possess MAO inhibitory properties will be presented and discussed in Chapter 4. The orientations in the pharmacophore models and the mapping of these drugs with the pharmacophore models will also be presented and discussed in Chapter 4.

Table 3.9. The drugs that were selected for *in vitro* evaluation as MAO-A and MAO-B inhibitors.

	Mapped to isoform		**Mapped to isoform**
Acetaminophen	A	Milrinone	A
Acyclovir	A	Minaprine	B
Anagrelide	A	Naproxen	B
Atenolol	A	Ondansetron	A
Betoxalol	B	Pantoprazole	B
Caffeine	A	Propranolol	B
Dantroline	B	R-(–)-Apomorphine	A
Esmolol	B	Ritodrine	B
Esomeprazole	B	Sulfanilamide	A
Ethambutol	B	Sulfisoxazole	A
Ethoxzolamide	A	Tolcapone	A
Flurbiprofen	B	Tolnaftate	B
Hesperetin	B	Tramadol	B
Leflunomide	B	Tolmetin	B
Midodrine	A/B		